WAVE PROPAGATION IN INFINITE PERIODIC STRUCTURES TAKING INTO ACCOUNT ENERGY ABSORPTION

Darryl McMahon

Maritime Division, Defence Science and Technology Group, HMAS Stirling, WA 6168, Australia
Email: darryl.mcmahon@dsto.defence.gov.au

Abstract

This paper explores the possibility of generalised periodic structure waves (PSW) that include the well-known Bloch-Floquet (BF) waves as a special case. We consider two types of structure waves (SW) in an infinite, uniform, one dimensional structure of equally spaced scatterers that also absorb energy. For the first structure wave type (SW1), forward transmission and backward reflection phase shifts are independent of wave propagation direction. For a second structure wave type (SW2), the phase shifts have opposite signs for opposite directions of propagation. Examples of SW1 are bending waves, such as flexural waves of a plate, and for SW2 longitudinal waves, such as acoustic waves in a fluid. The differences in amplitudes and phases of the forward and backward SW within any "cell" between adjacent scatterers are found to be equivalent to continuous PSW convolved with a periodic structure function. Finding the PSW dispersion relations requires a function that is the solution of a quadratic equation derived from imposing the same relative SW amplitudes and phases in all cells. Conservation of energy identifies physically acceptable PSW. For no energy absorption and backward and forward scatter phase shifts differing by $\pm\pi/2$, PSW of the first type (PSW1) are BF waves that propagate unattenuated in passing bands and are evanescent in stopping bands. Including energy absorption for the same phase shifts, PSW1 propagation occurs at all wavenumbers but is attenuated. This extends the BF dispersion relations to include energy absorption which blurs the distinction between passing and stopping bands. For other scatterer phase shifts, PSW1 may still be possible but only at discrete wavenumbers. In contrast PSW of the second type (PSW2) are only consistent with conservation of energy at discrete stopping wavenumbers that are the Bragg reflection condition. PSW1 also exhibit Bragg reflection, but as a narrow stopping band for small scatterer reflectivity and energy absorption. A theory for incoherent wave energy scattering in an infinite periodic structure is also developed, and its results for energy reflection, transmission and absorption are similar to those of PSW1 except for coherence effects.

1. Introduction

Wave equations where parameters, such as the phase speed, vary periodically arise in many systems of practical importance such as electric filters [1], vibrational energy transport through solid lattices [1], the electronic properties of solids [2, 3], mechanical vibration filters [4], acoustic scattering from ribbed cylinders [5], vibrational energy transport along ribbed plates and cylinders [6, 7], and sonic crystals [8]. The book by Brillouin [1] derives many results for wave propagation in periodic structures including solutions to Mathieu's and Hill's periodic wave equations.

Investigating the possibility of periodic structure waves (PSW) has a long history [1]. The importance of PSW increased with the discovery that the electronic properties of solids are governed by quantum mechanical waves in a periodic lattice of electron scatterers. Considering a periodic structure with an infinite number of equal width cells and a scatterer in each cell, a dispersion relation for the PSW can be derived from imposing the condition that the relative complex amplitudes of forward and backward waves are the same for all cells [2, 3]. The PSW identified in quantum mechanics exhibit passing bands and stopping bands, which for electrons are allowed and forbidden energy bands. These PSW are also known as Bloch waves for a 3-D lattice and as Bloch- Floquet (BF) waves for a 1-D periodic structure.

The PSW of the Bloch-Floquet type might not be the only possibility for every periodic structure. BF waves require scattering phase shifts independent of the underlying SW direction, which does not hold for instance for acoustic forward transmission and backward reflection by a fluid scatterer embedded in another fluid [9]. We define in this paper two classes of PSW, one we denote PSW1 where the phase shifts are independent of SW propagation direction, and the other PSW2 where the phase shifts have opposite signs for opposite SW propagation directions.

The scatterers are equally spaced parallel lines or planes in an infinite periodic structure of SW propagating at normal incidence along the x axis. For simplicity evanescent SW excited by the scatterers are not considered although a previous paper has included them for deriving the dispersion relation for Bloch-Floquet flexural waves of a ribbed plate [10].

Subsection 2.1 defines the complex amplitudes of the forward and backward SW within a cell and the constraint on them imposed by a cell equivalence condition. Implicit is the assumption that propagation to $x \to \infty$ and energy absorption by the scatterers is exactly balanced by an energy source at $x \to -\infty$ so that wave amplitudes are time independent. A function γ relates the amplitudes and phases of waves in all cells. γ is equivalent to a wave in the periodic structure however this wave property is only exists at spatial separations that are multiples of scatterer separation d. This is analogous to sound waves in a lattice where the waves are not continuous but only exist at the discrete lattice points. However subsection 2.1 shows that a continuous PSW can still be defined and that a convolution of the PSW with a periodic function is equivalent to the coherent superposition of SW scattered along the structure.

Subsection 2.2 discusses γ which is the solution of a quadratic equation. The same quadratic equation is found for PSW1 and PSW2 and only requires one complex function denoted $\hat{\Gamma}$. However $\hat{\Gamma}$ is a different function of scattering phases shifts, amplitudes and energy absorption for PSW1 and PSW2. Subsection 2.3 shows how PSW1 provide an extension to the BF wave dispersion relation by taking into account energy absorption. Subsection 2.4 demonstrates there are significant differences between PSW1 and PSW2.

Section 3 discusses wave energy reflection and penetration for an infinite periodic structure. These are quantified by a periodic structure reflectivity μ, energy transmission factor η, and energy absorption factor κ. As expected from the results of subsections 2.3 and 2.4, μ, η and κ differ significantly for PSW1 and PSW2. For comparison, incoherent wave energy flux relationships for an infinite periodic structure are derived in subsection 3.1 and define μ_E, η_E and κ_E. κ is an indicator (but not proof) of PSW consistency with energy conservation. In particular, if the scatterers do not absorb energy, then κ must be zero. Subsection 3.2 shows that PSW1 fulfill this condition at all wavenumbers provided the backward and forward scattering phase shifts differ by $\pm\pi/2$, whereas PSW2 are only correct at the discrete wavenumbers corresponding to Bragg reflection. κ_1 for PSW1 are also close to κ_E when the scatterers absorb energy and so probably conform with energy conservation.

2. Periodic Structure Waves

The periodic structure consists of an infinite number of cells each of length d. The 0th cell is the domain $0 \le x \le d$, 1st cell $d \le x \le 2d$, .., nth cell $nd \le x \le (n+1)d$, etc. The scatterer for the 0th cell is at

$x=0$, for the 1st cell $x=d$ etc. Omitting the harmonic time dependent factor $e^{-i\omega t}$, structure waves in the 0th cell originating from $x=0$ and $x=d$ have the waveforms

$$\begin{aligned} \xi_0(x) &= Ae^{ik_s x}; 0 \le x \le d \\ \xi_d(x) &= Be^{-ik_s(x-d)}; 0 \le x \le d \end{aligned} \tag{1}$$

where A and B are complex amplitudes and k_s is the SW wavenumber. The net waveform in the 0th cell is the superposition $w(x)=\xi_0(x)+\xi_d(x), 0 \le x \le d$.

For the purpose of defining in subsection 2.2 energy absorption by the scatterers, the energy flux for $\xi_0(x)$ is proportional to $|A|^2$ while the energy flux for $\xi_d(x)$ is proportional to $-|B|^2$ making the net energy flux in the 0th cell proportional to $|A|^2-|B|^2$.

2.1 Relation of continuous periodic structure waves to structure waves

Owing to the structure's periodicity, Eq. (1) applies to all cells except that the amplitudes for the nth cell become $A^{(n)}$ and $B^{(n)}$. The source of the structure waves is unspecified so one of the arbitrary amplitudes $A^{(n)}$ is used as a reference. So that the waveforms are identical in all cells, the ratio $B^{(n)}/A^{(n)}$ must be independent of n and hence equal to B/A for the 0th cell. It follows then that the amplitudes for all cells are related by[1]

$$A^{(n)} = A\gamma^n, B^{(n)} = B\gamma^n, n = 0, \pm 1, \ldots \tag{2}$$

where γ is a function to be determined from SW continuity where any two cells join.

How waveforms $f(x)=\gamma^n w(x-nd), nd \le x \le (n+1)d, n=0,\pm 1, \ldots$ relate to a PSW can be analysed by comparing the Fourier Transform (FT) of $f(x)$ with the FT of a single continuous wave $p(x)$. To avoid divergent integrals we restrict the FT analysis to the semi-infinite domain $x \ge 0$ where we assume $f(x)$ and $p(x)$ are finite. The single wave is

$$p(x) = e^{i\frac{\varphi}{d}x} \tag{3}$$

and[2] $\varphi = \varphi' + i\varphi''$ is a complex phase defined in $\gamma = e^{i\varphi}$. The phase of $p(x)$ is equivalent to a complex wavenumber $k_p = k' + ik''$ where $k' = \varphi'/d$ and $k'' = \varphi''/d$. From the periodic properties of $f(x)$

$$\begin{aligned} F(k) &= \int_0^\infty f(x) e^{-ikx} dx = W(k) G(k) \\ W(k) &= \int_0^d w(x') e^{-ikx'} dx' \\ G(k) &= \sum_{n=0}^\infty e^{in(\varphi - kd)} = \frac{1}{1-e^{i(\varphi-kd)}}, \varphi'' > 0 \end{aligned} \tag{4}$$

For $\varphi'' > 0$ the FT of $p(x)$ is finite and given by

$$P(k) = \int_0^\infty p(x) e^{-ikx} dx = -\frac{d}{i(\varphi - kd)} \tag{5}$$

---

[1] Applying the case n=1 to multiple adjacent pairs of cells establishes Eq. (2).

[2] Any complex quantity q is written as $q = q' + iq''$ where q' denotes the real part and q'' denotes the imaginary part.

Then from Eq. (4)

$$
\begin{aligned}
&G(k) = I(k)P(k) \\
&I(k) = \frac{1}{d}\frac{1}{1+\frac{1}{2!}[i(\varphi - kd)] + \dots \frac{1}{n!}[i(\varphi - kd)]^{n-1} + \dots} \\
&V(k) = W(k)I(k) \\
&F(k) = V(k)P(k)
\end{aligned}
\tag{6}
$$

From Eq. (6) the exact periodic structure function $f(x)$ is the convolution of a function $v(x)$ (the inverse FT of $V(k)$) and a continuous PSW $p(x)$:

$$
f(x) = \int_0^\infty v(x - x')p(x')dx', x \geq 0 \tag{7}
$$

Equation (7) is not the strong form of the Bloch theorem that $f(x)$ is proportional to $p(x)$. The Bloch theorem does hold however for discrete separations that are a multiple of d (i.e. $f(x+nd)/f(x) = p(x+nd)/p(x) = e^{inkd}$). Similarly, the simplified model of quantum waves in periodic potentials [2, 3] only satisfies the weaker version of the Bloch theorem Eq. (7).

2.2 Characteristic equation for periodic structure wave function γ

This paper assumes an infinite periodic structure where scatterers are defined by a forward scattering amplitude T and a backward scattering amplitude R. For simplicity, we omit evanescent waves that are generally excited at the boundary of two media. This leads to a quadratic (dubbed characteristic) equation for γ. More details for deriving the characteristic equation, including evanescent wave effects, are in reference [10].

T and R are complex where $T = |T|e^{i\phi}$ and $R = |R|e^{i\chi}$ where ϕ and χ are forward and backward scattering phase shifts. Forward transmission and backward reflection are constrained by $|T|^2 + |R|^2 = \sigma^2$ where $0 \leq 1 - \sigma^2 \leq 1$ is the proportion of energy absorbed by a scatterer from a single structure wave. We define $|T_0|$ by $|T| = \sigma|T_0|$ and $|R_0|$ by $|R| = \sigma|R_0|$ where $|T_0|^2 + |R_0|^2 = 1$. SW travelling in opposite directions and on opposite sides of scatterers in a periodic structure coherently interfere affecting the energy flux absorbed by scatterers in a complicated manner.

For both types of PSW, amplitudes A and B are related by two coupled homogeneous equations that in 2×2 matrix form have nontrivial solutions only if the matrix determinant is zero [10]. This leads to the quadratic equation

$$
\hat{\gamma}^2 - 2\hat{\Gamma}\hat{\gamma} + 1 = 0 \tag{8}
$$

For PSW1 $\hat{\gamma} = \gamma$ and

$$
\hat{\Gamma} = \frac{1}{2}\left(\left(1 - \frac{\hat{R}^2}{\hat{T}^2}\right)\hat{T} + \frac{1}{\hat{T}}\right) \tag{9}
$$

where $\hat{T} = e^{ik_s d}T$ and $\hat{R} = e^{ik_s d}R$. For PSW2 $\hat{\gamma} = \gamma e^{-i\phi}$ and

$$\hat{\Gamma}=\frac{1}{2}\left(\left(1-\frac{|R|^2}{|T|^2}\right)\hat{T}e^{-i\phi}+\frac{1}{\hat{T}e^{-i\phi}}\right) \tag{10}$$

Note that PSW1 and PSW2 are the same PSW for $\chi=\phi=0$ since the SW direction is then irrelevant.

Equation (8) factorises into

$$\left(\hat{\gamma}-e^{i\hat{\varphi}}\right)\left(\hat{\gamma}-e^{-i\hat{\varphi}}\right)=0 \tag{11a}$$

where the two solutions $e^{\pm i\hat{\varphi}}$ are PSW travelling in opposite directions, and

$$\frac{1}{2}\left(e^{i\hat{\varphi}}+e^{-i\hat{\varphi}}\right)=\hat{\Gamma} \tag{11b}$$

The complex phase $\hat{\varphi}$ defines a complex wavenumber $\hat{k}=\hat{k}'+i\hat{k}''$ by $\hat{\varphi}=\hat{k}d$ that relates to the complex wavenumber $k_p=k'+ik''$ defined in subsection 2.1 by $k_p=\hat{k}$ for a PSW1, and since for a PSW2 $\hat{\gamma}=\gamma e^{-i\phi}$, $k_p=\hat{k}+\phi/d$.

If $\hat{\varphi}$ has an imaginary part, one PSW solution from Eq. (11a) has decreasing amplitude with *x* and the other an increasing amplitude with *x*. This apparent asymmetry is merely a consequence of the arbitrary choice for the +*x* axis direction (i.e. an amplitude increase in one direction is a decrease in the opposite direction) so the two solutions of Eq. (11a) are two perspectives on the same PSW.

Equation (11b) can be solved for $\hat{\varphi}'$ and $\hat{\varphi}''$ in terms of $\hat{\Gamma}'$ and $\hat{\Gamma}''$ to obtain the dispersion relation and attenuation of PSW. $\hat{\varphi}'$ can be eliminated using the identity $\cos^2(\hat{\varphi}')+\sin^2(\hat{\varphi}')=1$, and this leads to a quadratic equation for a function $\hat{\Delta}$ defined by

$$\hat{\Delta}=\frac{1}{2}\left(e^{-2\hat{\varphi}''}+e^{2\hat{\varphi}''}\right)\geq 1 \tag{12}$$

Only one solution for $\hat{\Delta}$ is consistent with the inequality of Eq. (12) and is

$$\hat{\Delta}=\left(\hat{\Gamma}'^2+\hat{\Gamma}''^2\right)+\sqrt{\left(1-\left(\hat{\Gamma}'^2+\hat{\Gamma}''^2\right)\right)^2+4\hat{\Gamma}''^2} \tag{13}$$

$e^{\pm 2\hat{\varphi}''}$ are easily derived in terms of $\hat{\Delta}$ from Eq. (12), and hence $e^{\pm\hat{\varphi}''}$ are found to be

$$e^{\pm\hat{\varphi}''}=\sqrt{\frac{\left(\hat{\Delta}+1\right)}{2}}\pm\sqrt{\frac{\left(\hat{\Delta}-1\right)}{2}} \tag{14}$$

Using Eqs. (11b) and (12), $\hat{\varphi}'$ is then obtained from

$$\cos(\hat{\varphi}')=\frac{\hat{\Gamma}'}{\sqrt{\frac{\left(\hat{\Delta}+1\right)}{2}}},\sin(\hat{\varphi}')=-\frac{\hat{\Gamma}''}{\sqrt{\frac{\left(\hat{\Delta}-1\right)}{2}}} \tag{15}$$

Figure 1 compares plots of $\hat{\Delta}$, $e^{-\hat{\varphi}''}$, $\cos(\hat{\varphi}')$ and $\sin(\hat{\varphi}')$ versus one cycle of positive $\hat{\Gamma}'$ for different constant positive values of $\hat{\Gamma}''$. Negative $\hat{\Gamma}'$ and $\hat{\Gamma}''$ only affect $\cos(\hat{\varphi}')$ and $\sin(\hat{\varphi}')$ and do not convey more information. A sharp transition is seen at $\hat{\Gamma}' = 1, \hat{\Gamma}'' = 0$ in every plot. For $\hat{\Gamma}' \le 1, \hat{\Gamma}'' = 0$ the PSW is a propagating wave if $|B/A| \ne 1$, such as a Bloch-Floquet wave in a passing band, or standing wave if $|B/A| = 1$. An evanescent wave exists for $\hat{\Gamma}' > 1, \hat{\Gamma}'' = 0$ and corresponds to a Bloch-Floquet stopping band. In a stopping band $\hat{\varphi}''$ varies with $\hat{\Gamma}'$, and $\hat{\varphi}'$ is a integer multiple of π. Discrete wavenumber solutions also exist for $\hat{\Gamma}'' = 0$ and are discussed in Section 3.

For $\hat{\Gamma}'' \ne 0$ (see Fig.1 curves for $\hat{\Gamma}'' = 0.5$ and $\hat{\Gamma}'' = 1$), there is no sharp transition from an unattenuated passing band to a stopping band but rather an attenuated PSW exists for all $\hat{\Gamma}'$. There is a smooth transition near $\sqrt{\hat{\Gamma}'^2 + \hat{\Gamma}''^2} = 1$ where the passing band is replaced by an attenuated wave band for $\sqrt{\hat{\Gamma}'^2 + \hat{\Gamma}''^2} < 1$ and the stopping band becomes propagating for $\sqrt{\hat{\Gamma}'^2 + \hat{\Gamma}''^2} > 1$ but more strongly attenuated. The conditions $\sqrt{\hat{\Gamma}'^2 + \hat{\Gamma}''^2} << 1$ and $\sqrt{\hat{\Gamma}'^2 + \hat{\Gamma}''^2} >> 1$ approximate BF wave passing and stopping bands respectively where the effect of $\hat{\Gamma}'' \ne 0$, due to energy absorption by the scatterers for instance, is negligible.

2.3 PSW1 dispersion relations and attenuation

$\hat{\Gamma}'$ and $\hat{\Gamma}''$ determine the dispersion relations and amplitudes of all PSW as shown by Eqs. (13), (14) and (15). However the ranges of $\hat{\Gamma}'$ and $\hat{\Gamma}''$ are limited by the type of PSW. For PSW1 from Eq. (9) we find

$$\begin{aligned} \hat{\Gamma}' &= \frac{1}{\sigma|T_0|}(1-u)\cos(k_s d + \phi) + \frac{1}{\sigma|T_0|} v \sin(k_s d + \phi) \\ \hat{\Gamma}'' &= -\frac{1}{\sigma|T_0|} v \cos(k_s d + \phi) - \frac{1}{\sigma|T_0|} u \sin(k_s d + \phi) \end{aligned} \tag{16}$$

where

$$\begin{aligned} u &= \frac{1}{2}\left(1 - \sigma^2 + \sigma^2 |R_0|^2 (1 + \cos(2(\chi - \phi)))\right) \\ v &= \frac{1}{2}\sigma^2 |R_0|^2 \sin(2(\chi - \phi)) \end{aligned} \tag{17}$$

For $\sigma = 1, \chi - \phi = \pm\pi/2$ we obtain $u = 0, v = 0$ which makes $\hat{\Gamma}'' = 0$ for all SW wavenumbers k_s, leading to unattenuated BF waves in a passing band and evanescent BF waves in a stopping band. From Eq. (16), $\hat{\Gamma}'' = 0$ is also possible for $u \ne 0, v \ne 0$ at a discrete wavelength, corresponding to PSW1 that are unattenuated with $|\gamma_1^{(-)}| = 1, \hat{\varphi}_1'' = 0, \hat{\varphi}_1' < \pi$, attenuated with $|\gamma_1^{(-)}| < 1, \hat{\varphi}_1'' > 0, \hat{\varphi}_1' < \pi$ or evanescent for $|\gamma_1^{(-)}| < 1, \hat{\varphi}_1'' > 0, \hat{\varphi}_1' = \pi$. Since unattenuated PSW1solutions exists for $\sigma \ne 1$, they are only consistent with energy conservation if the SW at the scatterers coherently interfere to make a null so that no energy is absorbed.

Figure 2 shows plots of the dispersion relation $\hat{\varphi}_1'$ (A) and amplitude $|\gamma_1^{(-)}| = e^{-\hat{\varphi}_1''}$ (B) for PSW1 in the case $\chi - \phi = \pm\pi/2, v = 0$ for weak (curves 1, 2 and 3) and strong (curves 4 and 5) energy absorption by the scatterers. Curves 1 and 2 with negligible energy absorption exhibit Bloch-Floquet passing and stopping bands. Contrasting curves 2 and 3 shows that small energy absorption by the scatterers only affects the dispersion relation close to the passing band and stopping band transition but observing this effect on a propagating PSW1 experimentally may be made more difficult by the decrease of wave amplitude close to the transition.

2.4 PSW2 dispersion relations and attenuation

From Eq. (10) we find

$$\begin{aligned}\hat{\Gamma}' &= \frac{1}{2\sigma|T_0|}\left(\left(2|T_0|^2-1\right)\sigma^2+1\right)\cos\left(k_s d\right)\\ \hat{\Gamma}'' &= \frac{1}{2\sigma|T_0|}\left(\left(2|T_0|^2-1\right)\sigma^2-1\right)\sin\left(k_s d\right)\end{aligned} \tag{18}$$

Unlike a PSW1, $\hat{\Gamma}$ does not depend on either ϕ or χ. Also unlike a PSW1, $\hat{\Gamma}''=0$ for a PSW2 only occurs at the discrete wavenumbers $\sin\left(k_s d\right)=0, \cos\left(k_s d\right)=\pm 1$.

Figure 3 shows plots of PSW2 dispersion relation $\hat{\varphi}_2'$ (A) and amplitude $\left|\gamma_2^{(-)}\right| = e^{-\hat{\varphi}_2''}$ (B) versus $k_s d$. The corresponding curves in Figs. 2 and 3 have the same values of $|T_0|$ and σ and show that PSW2 are much more attenuated than PSW1 around middle wavenumbers but much less attenuated at the ends $\sin\left(k_s d\right)\to 0, \cos\left(k_s d\right)\to \pm 1$. Another difference is that the PSW1 phase $\hat{\varphi}_1'$ can have values anywhere between 0 and π provided $\chi-\phi=\pm\pi/2$ whereas the PSW2 phase $\hat{\varphi}_2'$ is restricted to a narrower range provided $\sigma \ge 1/\sqrt{2}$.

3. Energy Reflection, Transmission and Absorption by Infinite Periodic Structures

This section develops the theory for wave energy fluxes in infinite periodic structures. Formulae for wave energy reflection by and penetration into a structure are derived. Energy penetration past one scatterer layer is then divided into a propagation part and an absorption part. The absorption part allows a limited test whether PSW parameters conform to conservation of energy.

3.1 Incoherent wave energy reflection, transmission and absorption

A characteristic equation for incoherent wave energy fluxes in an infinite periodic structure is similar to the characteristic equation for coherent PSW. An energy flux version of cell independence is

$$\left|A^{(n)}\right|^2 = |A|^2\left(|\gamma|^2\right)^n, \left|B^{(n)}\right|^2 = |B|^2\left(|\gamma|^2\right)^n, n=0,\pm 1,\ldots \tag{19}$$

where $|\gamma|^2$ is a periodic structure function for energy flux. The coupled equations for forward and backward fluxes in the 0$^{\text{th}}$ cell are

$$\begin{pmatrix} -\sigma^2|R_0|^2 & \left(1-\sigma^2|T_0|^2|\gamma|^2\right) \\ \left(|\gamma|^2-\sigma^2|T_0|^2\right) & -\sigma^2|R_0|^2|\gamma|^2 \end{pmatrix}\begin{pmatrix}|A|^2\\ |B|^2\end{pmatrix} = \begin{pmatrix}0\\0\end{pmatrix} \tag{20}$$

Setting the determinant of the 2×2 matrix to zero, we find the quadratic equation for $|\gamma|^2$

$$|\gamma|^4 - \frac{1+\left(\sigma^2|T_0|^2\right)^2-\left(\sigma^2|R_0|^2\right)^2}{\sigma^2|T_0|^2}|\gamma|^2+1=0 \tag{21}$$

Equation (21) has the two solutions

$$\left|\gamma_E^{(\pm)}\right|^2 = \frac{1}{2\sigma^2|T_0|^2}\left(2\sigma^4|T_0|^2 + 1 - \sigma^4 + (\pm)2\sigma^2\sqrt{1-\sigma^4}\sqrt{\left(\frac{1-\sigma^2}{2\sigma^2}+|T_0|^2\right)\left(\frac{1+\sigma^2}{2\sigma^2}-|T_0|^2\right)}\right) \tag{22}$$

that are equivalent versions of energy propagation and absorption along the structure. $\left|\gamma_E^{(\pm)}\right|^2 = 1$ for $\sigma = 1$ is the expected equal flux in all cells if scatterers do not absorb energy. For $|T_0| = 1$, $\left|\gamma_E^{(-)}\right|^2 = \sigma^2$ and $\left|\gamma_E^{(+)}\right|^2 = 1/\sigma^2$ as expected if the scatterers only absorb energy.

From Eq. (20) the ratio of backward and forward energy fluxes is

$$\frac{\left|B_E^{(\pm)}\right|^2}{\left|A_E^{(\pm)}\right|^2} = \frac{\sigma^2|R_0|^2}{1-\sigma^2|T_0|^2\left|\gamma_E^{(\pm)}\right|^2} \tag{23}$$

Using Eq. (20) and $\left|\gamma_E^{(-)}\right|^2 \le 1$, the incoherent wave reflectivity $0 \le \mu_E \le 1$ of the structure is

$$\mu_E = \frac{\left|B_E^{(-)}\right|^2}{\left|A_E^{(-)}\right|^2} = \frac{\sigma^2|R_0|^2}{1-\sigma^2|T_0|^2\left|\gamma_E^{(-)}\right|^2} \tag{24}$$

Substituting $\sigma = 1$ and $\left|\gamma_E^{(-)}\right|^2 = 1$ into Eq. (24) gives $\mu_E = 1$ since $|R_0|^2$ cancels out but this is incorrect if $|R_0| = 0$ because $\mu_E = 0$ is expected for one just implicit energy source and at $x \to -\infty$. This discontinuity of μ_E in the limit $\sigma \to 1$ is avoided if σ is at least infinitesimally smaller than 1.

The net flux in the forward direction is proportional to $1-\mu_E$ which consists of propagation through the structure and the absorption by the scatterers. The proportion of the net flux incident onto a scatterer that is still a forward net flux in the next cell is

$$\eta_E = \left|\gamma_E^{(-)}\right|^2 (1-\mu_E) \tag{25}$$

and the proportion of the net flux that is absorbed by the scatterer is

$$\kappa_E = \left(1-\left|\gamma_E^{(-)}\right|^2\right)(1-\mu_E) \tag{26}$$

η_E is a measure of wave energy penetration by propagation and κ_E is a measure of wave energy penetration by absorption. Note that $\mu_E + \eta_E + \kappa_E = 1$ by conservation of energy.

3.2 Coherent PSW energy reflection, transmission and absorption

PSW formulae for μ, η and κ apply the same definitions Eqs. (24), (25) and (26) but incorporate wave coherence. In the case of PSW1, we find

$$\mu_1 = \frac{\sigma^2|R_0|^2}{1+\sigma^2|T_0|^2\left|\gamma_1^{(-)}\right|^2 - 2\sigma|T_0|\left|\gamma_1^{(-)}\right|\cos(k_s d + \phi + \hat{\varphi}_1')} \tag{27}$$

and in the case of PSW2

$$\mu_2 = \frac{\sigma^2 |R_0|^2}{1+\sigma^2 |T_0|^2 \left|\hat{\gamma}_2^{(-)}\right|^2 - 2\sigma |T_0| \left|\hat{\gamma}_2^{(-)}\right| \cos\left(k_s d + \hat{\varphi}_2'\right)} \tag{28}$$

For both types of PSW,

$$\eta_n = \left|\gamma_n^{(-)}\right|^2 (1-\mu_n), \kappa_n = \left(1-\left|\gamma_n^{(-)}\right|^2\right)(1-\mu_n), n = 1,2 \tag{29}$$

Figures 4 and 5 compare side-by-side PSW1, PSW2 and incoherent wave energy flux results for μ and κ using identical values of σ and $|T_0|$. The PSW1 results are only symmetric around SW1 phase shift corrected wavenumber $k_s d + \phi = \pi/2$ by setting $\chi - \phi = \pm\pi/2$. The discontinuity of μ at $\sigma = 1$ is avoided in these plots by using a maximum σ of 0.999. Curves 1 and 2 differ from curves 3, 4 and 5 by having almost negligible energy absorption by the scatterers. In Fig. 4 μ_E differs significantly from μ_1 and μ_2 for curves 1 and 2 whereas in Fig. 5 κ_1 and κ_E are fairly close while κ_2 is significantly different from κ_E. Overall κ_E is much closer to κ_1 than κ_2 and is almost equal to κ_1 for large energy absorption curves 4 and 5. Except for $k_s = \pi/d$, it is clear that PSW2 are not consistent with energy conservation since $\sigma \to 1$ does not give $\kappa_2 \to 0$.

Whereas $\mu_2 \to 1$ at the wavenumber $k_s = \pi/d$ for a range of σ values, for a PSW1 $\mu_1 \to 1$ is over a stopping band which only approaches a discrete wavenumber $k_s = (\pi - \phi)/d$ for very low back reflection coefficient $|R_0| \to 0$ and low energy absorption factor $1-\sigma^2 \to 0$. These discrete wavenumbers are examples of the Bragg condition for strong reflection by a periodic structure. In Fig. 4 B, $\mu_2 \to 1$ is the case of Bragg reflection at a SW2 wavelength equal to 2*d*. In comparison, Fig. 4A $\mu_1 \to 1$ is Bragg reflection at a SW1 wavelength equal to $2d/(1-\phi/\pi)$. The effect of the forward scattering phase shift becomes relatively smaller for shorter wavelength Bragg reflections at SW1 wavelengths $2d/(n-\phi/\pi), n = 1,2,\ldots$

Figure 6 demonstrates for PSW1 the effect of $v \neq 0$ by setting the scatterer forward transmission and backward reflection phase difference to $\chi - \phi = \pm\pi/2.5$. In Fig. 6A, curves 1 and 2 exhibit $\hat{\Gamma}'' = 0$ and $\left|\gamma_1^{(-)}\right| = 1, \hat{\varphi}_1'' = 0$ of an unattenuated PSW1 at just one wavenumber, compared to Fig. 2B curves 1 and 2 with unattenuated PSW1 over a passing band. Since in Fig. 6B $\kappa_1 \to 0$ at these discrete wavenumbers, energy is unambiguously conserved. For all other wavenumbers Fig. 6B curves 1 and 2 show that $\kappa_1 \neq 0$ and so are not consistent with energy conservation. Curve 3 is the same as curve 2 except that the energy absorption factor $1-\sigma^2$ is larger which shifts where $\hat{\Gamma}'' = 0$ to a different discrete wavenumber. At this wavenumber the PSW1is propagating (since $\hat{\varphi}_1' < \pi$) and is unattenuated since $\left|\gamma_1^{(-)}\right| = 1, \hat{\varphi}_1'' = 0$. This is physically meaningful only if there is no energy absorbed by the scatterers, such as a SW null at the scatterers. However Fig. 6B curve 3 shows that κ_1 is a small but nonzero minimum contrary to energy conservation. Curve 4 is the same as curve 3 except with greater scatterer energy absorption factor $1-\sigma^2$ and a larger nonzero minimum in κ_1. Finally curve 5 for large scatterer energy absorption factor $1-\sigma^2$ shows strong PSW1 attenuation at all wavenumbers including the wavenumber where $\hat{\Gamma}'' = 0$ and $\left|\hat{\Gamma}'\right| > 1, \left|\gamma_1^{(-)}\right| < 1, \hat{\varphi}_1'' > 0, \hat{\varphi}_1' = \pi$. Since the PSW1 is attenuated, an unambiguous violation of energy conservation is not clear from κ_1 for curve 5.

4. Conclusions

This paper explored wave reflection, propagation and absorption in an infinite 1-D structure of equally spaced scatterers. Two types of periodic structure waves, PSW1 and PSW2, have been analysed. Only PSW1 for $\chi - \phi = \pm\pi/2$ give results that conform with conservation of energy where it can be unambiguously tested in the case $\sigma \to 1$. Also κ_1 for $\chi - \phi = \pm\pi/2$ and $\sigma < 1$ are approximated by incoherent wave κ_E in a periodic structure. For these reasons, PSW1 for $\chi - \phi = \pm\pi/2$ are likely to correctly extend the dispersion relations for Bloch-Floquet waves to take into account energy absorption. This extension shows that energy absorption removes the sharp distinction between passing and stopping bands of BF waves.

For $\chi - \phi \neq \pm\pi/2$, PSW1 only conform with conservation of energy in the case $\sigma \to 1$ at a discrete wavenumber. PSW2 conform with energy conservation in the case $\sigma \to 1$ at a discrete wavenumber that happens to be the Bragg reflection condition. These are probably limitations of the simplifying approximations for PSW in terms of forward and backward scattering amplitudes. A older example of the scattering method's shortfall is that the strong form of the Bloch theorem is not satisfied for quantum waves in a periodic potential [2, 3]. The method may be improved for PSW1 by including $\chi - \phi$, $|R_0|$ and σ mutual dependence on wavenumber. However $\hat{\Gamma}$ for PSW2 does not depend on χ or ϕ reducing the flexibility to make it conform with energy conservation. Inclusion of evanescent waves that correlate wave continuity constraints at neighboring scatterers [10] may reduce some of the current limitations of a scattering theory for PSW. It is premature to conclude that the only realistic PSW that can exist are PSW1 for $\chi - \phi = \pm\pi/2$.

Acknowledgement

This research was supported by an Honorary Fellowship from DST Group and an Adjunct Fellowship from Curtin University CMST.

References

[1] Brillouin, L. *Wave Propagation in Periodic Structures*, Second Edition, Dover Publications, Inc., 1953.

[2] Kittel, C. *Introduction to Solid State Physics*, Eighth Edition, John Wiley & Sons, 2004.

[3] Ashcroft, N.W. and Mermin, N.D. *Solid State Physics*, Holt, Rinehart and Winston, 1976.

[4] Cremer, L., Heckl, M. and Ungar, E.E. *Structure Borne Sound*, second edition, Springer-Verlag, pp. 405–415, 1973.

[5] Plotinus, D.M., Bucaro, J.A. and Houston, B.H. "Scattering from flexural waves on a ribbed cylindrical shell", *Journal of the Acoustical Society of America*, **96**, 2785–2790, (1994).

[6] Hodges, C.H. and Woodhouse, J. "Theories of noise and vibration transmission in complex structures", *Report on Progress in Physics*, **49**, 107–170, (1986).

[7] Sorokin, S.V. and Ershova, O.A. "Plane wave propagation and frequency band gaps in periodic plates and cylindrical shells with and without heavy fluid loading", *Journal of Sound and Vibration*, **278**(3), 501–526, (2004).

[8] Miyashita, T. "Sonic crystals and sonic wave-guides", *Measurement Science and Technology*, **16**, R47–R63, (2005).

[9] Blackstock, D. T., *Fundamentals of Physical Acoustics*, John Wiley and Sons, pp. 163–167, 2000.

[10] McMahon, D. "Bloch-Floquet flexural waves for an infinite ribbed plate including near field effects", *Proceedings of the 22nd International Congress on Sound and Vibration* (ICSV22), Florence, Italy, 12-16 July 2015.

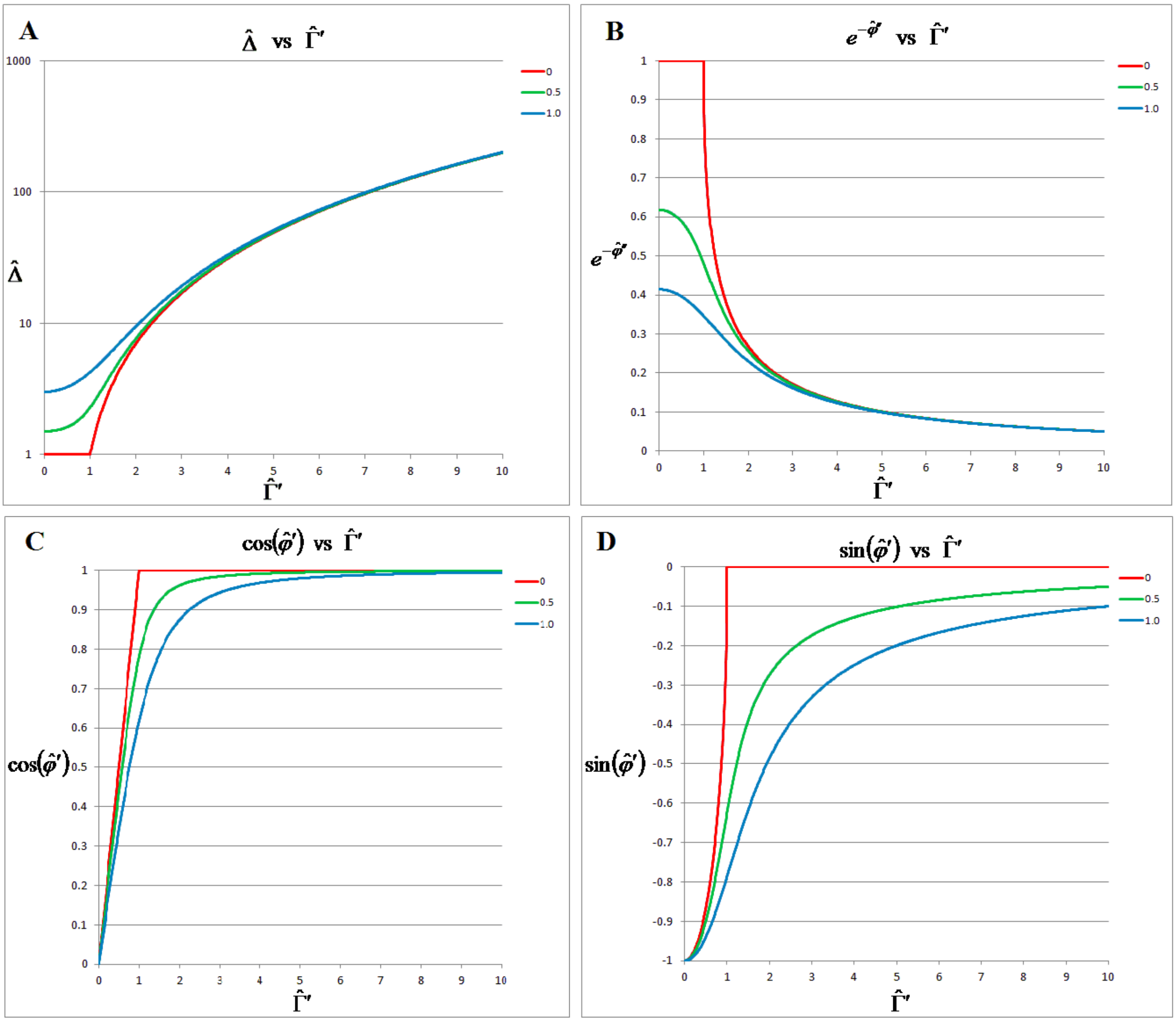

Figure 1. Plots of components of PSW functions versus positive $\hat{\Gamma}'$ for positive values of $\hat{\Gamma}''$ equal to 0, 0.5 and 1.0. A. $\hat{\Delta}$, B. $e^{-\hat{\varphi}''}$, C. $\cos(\hat{\varphi}')$ and D. $\sin(\hat{\varphi}')$

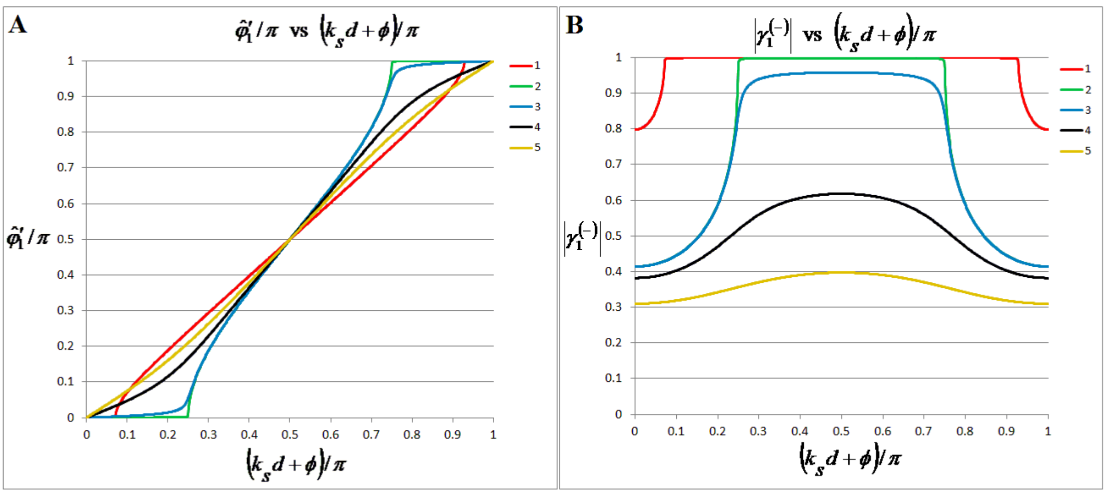

Figure 2. Plots of PSW1 dispersion relations (A) and amplitudes (B) versus the phase shift corrected structure wave wavenumber, $\chi-\phi=\pi/2$ 1. $|T_0|=0.975, \sigma=0.999$, 2. $|T_0|=1/\sqrt{2}, \sigma=0.999$, 3. $|T_0|=1/\sqrt{2}, \sigma=0.97$, 4. $|T_0|=1/\sqrt{2}, \sigma=1/\sqrt{2}$, 5. $|T_0|=1/\sqrt{2}, \sigma=0.5$

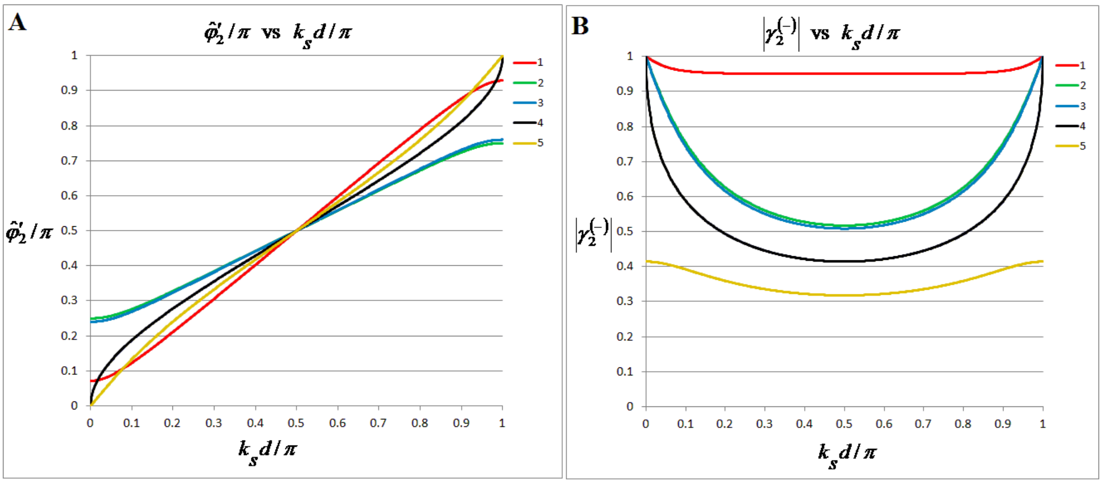

Figure 3. Plots of PSW2 dispersion relations (A) and amplitudes (B) versus the structure wave wavenumber. 1. $|T_0| = 0.975, \sigma = 0.999$, 2. $|T_0| = 1/\sqrt{2}, \sigma = 0.999$, 3. $|T_0| = 1/\sqrt{2}, \sigma = 0.97$, 4. $|T_0| = 1/\sqrt{2}, \sigma = 1/\sqrt{2}$, 5. $|T_0| = 1/\sqrt{2}, \sigma = 0.5$

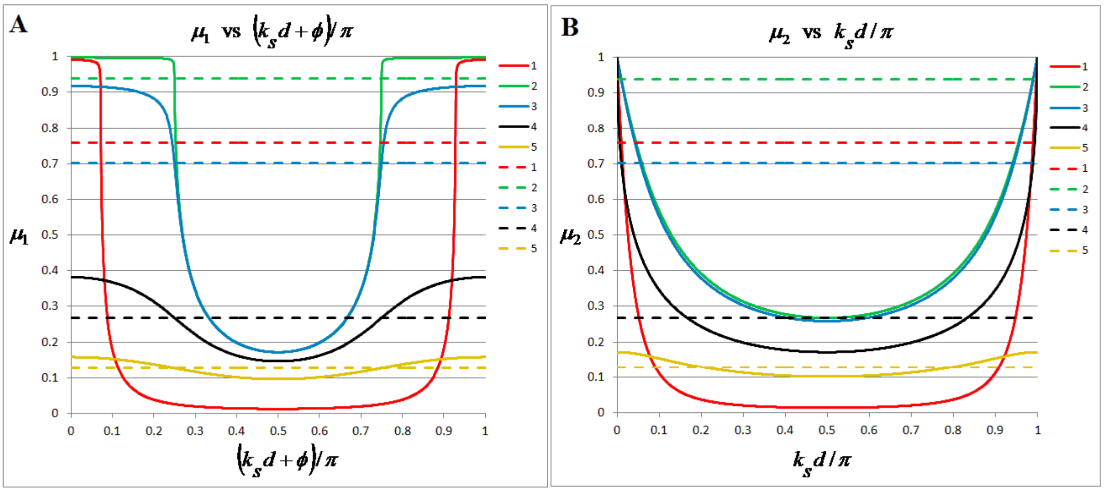

Figure 4. Comparison of periodic structure energy reflection factors μ_1, μ_2 and μ_E (dashed lines) for PSW1 ($\chi - \phi = \pi/2$) and PSW2 versus their respective structure wavenumbers. 1. $|T_0| = 0.975, \sigma = 0.999$, 2. $|T_0| = 1/\sqrt{2}, \sigma = 0.999$, 3. $|T_0| = 1/\sqrt{2}, \sigma = 0.97$, 4. $|T_0| = 1/\sqrt{2}, \sigma = 1/\sqrt{2}$, 5. $|T_0| = 1/\sqrt{2}, \sigma = 0.5$

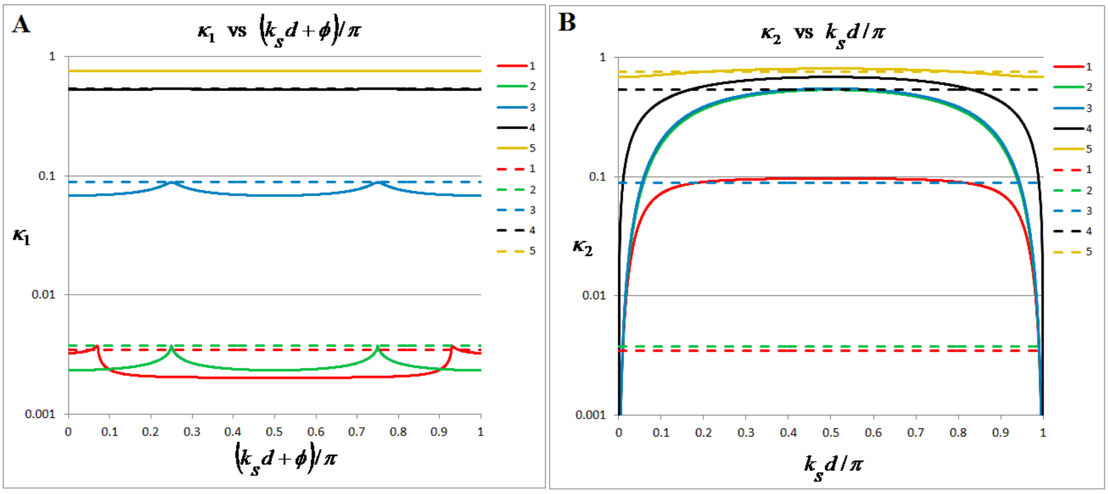

Figure 5. Comparison of periodic structure energy absorption factors κ_1, κ_2 and κ_E (dashed lines) for PSW1($\chi - \phi = \pi/2$) and PSW2 versus their respective structure wavenumbers. 1. $|T_0| = 0.975, \sigma = 0.999$, 2. $|T_0| = 1/\sqrt{2}, \sigma = 0.999$, 3. $|T_0| = 1/\sqrt{2}, \sigma = 0.97$, 4. $|T_0| = 1/\sqrt{2}, \sigma = 1/\sqrt{2}$, 5. $|T_0| = 1/\sqrt{2}, \sigma = 0.5$

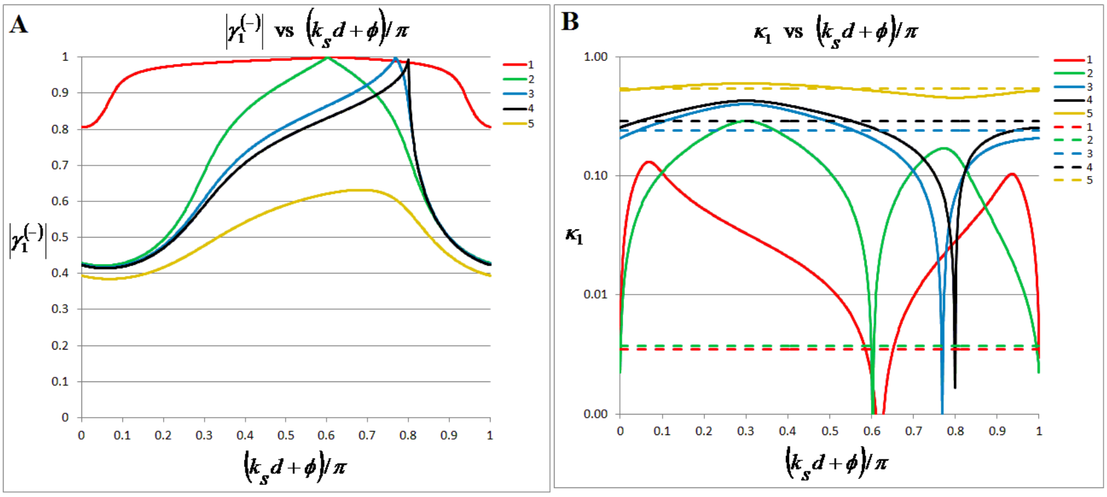

Figure 6. Plots of $\left|\gamma_1^{(-)}\right|$ (A), κ_1 (B) for PSW1 ($\chi-\phi=\pi/2.5$) and κ_E (dashed lines) versus the phase shift corrected wavenumber of the structure waves. 1. $|T_0|=0.975, \sigma=0.999$, 2. $|T_0|=1/\sqrt{2}, \sigma=0.999$, 3. $|T_0|=1/\sqrt{2}, \sigma=0.9$, 4. $|T_0|=1/\sqrt{2}, \sigma=0.8745$, 5. $|T_0|=1/\sqrt{2}, \sigma=1/\sqrt{2}$